

Atmospheric Fate of Chlorobromomethane: Rate Constant for the Reaction with OH, UV Spectrum, and Water Solubility

Vladimir L. Orkin,^{*,†,‡} Victor G. Khamaganov,[‡] Andrey G. Guschin,[‡] Robert E. Huie,[†] and Michael J. Kurylo[†]

Physical and Chemical Properties Division, National Institute of Standards and Technology, Gaithersburg, Maryland 20899, and Institute of Energy Problems of Chemical Physics, Russian Academy of Sciences, Moscow 117829, Russia

Received: August 9, 1996; In Final Form: October 24, 1996[⊗]

The rate constant for the reaction of CH₂ClBr with OH was measured by both flash photolysis resonance fluorescence and discharge flow electron paramagnetic resonance techniques over the temperature range 277–370 K. The Arrhenius expression $3.04_{-0.6}^{+0.8} \times 10^{-12} \exp\{-(978 \pm 72)/T\}$ cm³ molecule⁻¹ s⁻¹ was derived from a composite fit to both data sets. Absorption cross-sections of CH₂ClBr were measured from 187 to 290 nm at 295 K. The solubility of CH₂ClBr in water was also estimated to determine if such a process could be important in determining the atmospheric lifetime of CH₂ClBr. The atmospheric lifetime and ozone depletion potential for CH₂ClBr were estimated.

Introduction

Chlorobromomethane (CBM) is a natural source gas, formed by algal biological processes, which delivers bromine into Earth's atmosphere.¹ However, the limited measurements of the atmospheric abundance of CH₂ClBr vary widely. Rasmussen and Khalil² reported approximately 2.2 pptv in the Arctic with a uniform height distribution up to 7 km, while Class and Ballschmiter³ reported 0.4 pptv for the mean concentration over 30 °S to 40 °N. In spite of its lower concentration than the main source of atmospheric bromine, CH₃Br (10–15 pptv),⁴ CBM and other organic bromides can influence the reactive bromine budget in the atmosphere, depending on their efficiency of bromine release via both chemical reactions and solar ultraviolet photolysis. Additional interest in chlorobromomethane stems from its effectiveness as a cleaning agent in industrial applications⁵ and as a possible fire suppressant. In order to better quantify the atmospheric behavior of this compound, we have determined the rate constant for its reaction with OH and have measured its UV absorption spectrum. We have also estimated the solubility of CH₂ClBr in water since oceanic or rainout losses can possibly provide other sink mechanisms. Rate constant measurements were carried out in two different institutions by two different techniques using the same purified CBM sample in order to improve the reliability of the data upon which atmospheric lifetimes are based.

Experimental Section²⁶

Detailed descriptions of the apparatuses and the experimental methods employed in the studies of the reaction between OH and CH₂ClBr are given in previous papers.^{6–14} Therefore, only brief descriptions are given here.

The principal component of the flash photolysis/resonance fluorescence (FP/RF) apparatus is a Pyrex reactor (of approximately 50 cm³ internal volume) thermostated with water or methanol circulated through its outer jacket. The reaction was studied in argon carrier gas (99.9995% purity) at a total pressure of 100.0 Torr (13.33 kPa). Flows of dry argon, argon bubbled through water thermostated at 276 K, and CH₂ClBr (0.5–2.0% mixture diluted with argon) were premixed and

flowed through the reactor at a total flow rate between 0.08 and 1.6 cm³(STP) s⁻¹. Various CH₂ClBr/argon mixtures were used to verify that the dilution process did not introduce any systematic error into the rate constant measurement. The concentration of CH₂ClBr in the bulb mixtures was verified by UV absorption measurements to be correct within 1%. The concentrations of the gases in the reactor were determined by measuring the mass flow rates and the total pressure using an MKS Baratron manometer. Flow rates of both argon and the H₂O/argon mixture were measured using calibrated Tylan mass flow meters, whereas that of the CH₂ClBr/argon mixture was determined by direct measurements of the rate of pressure change in a calibrated volume. Hydroxyl radicals were produced by the pulsed photolysis (0.2–4 Hz repetition rate) of H₂O (introduced via the 276 K argon/H₂O bubbler) using a xenon flash lamp focused into the reactor. The radicals were then monitored by their resonance fluorescence near 308 nm, excited by a microwave-discharge resonance lamp (2.1 Torr or 280 Pa of a ca. 2% mixture of H₂O in ultrahigh-pressure helium) focused into the reactor center. The resonance fluorescence signal was recorded on a computer-based multichannel scaler (channel width 100 μs) as a summation of 2000–15 000 consecutive flashes. The radical decay signal at each reactant concentration ([CBM]) was analyzed as described by Orkin et al.¹⁰ to obtain the first-order decay rate due to the reaction under study (τ_{CBM}^{-1}).

The principal component of the discharge flow/electron paramagnetic resonance (DF/EPR) apparatus is a quartz tubular reactor of 2.0 cm i.d. internally coated with a fluorocarbon varnish (F-46) to reduce wall loss of OH and to prevent heterogeneous reactions. The temperature of the reactor was controlled (± 0.2 K) with water circulated through its outer jacket. Hydrogen atoms were generated by a microwave discharge in an H₂/He mixture and OH radicals produced near the end of the movable injector by the fast reaction between H atoms and NO₂. The reactant (CH₂ClBr) and NO₂ were supplied to the flow reactor upstream from the injector tip as admixtures in helium carrier gas (99.999% purity) and were always in large excess over OH. The concentration of hydroxyl radicals at the end of the flow reactor was monitored using electron paramagnetic resonance spectroscopy. The initial OH concentrations in this study were 2×10^{11} to 2×10^{12} molecules·cm⁻³. The linear flow velocities in the reactor were 600–1500 cm·s⁻¹, at

[†] National Institute of Standards and Technology.

[‡] Russian Academy of Sciences.

[⊗] Abstract published in *Advance ACS Abstracts*, December 15, 1996.

a total gas pressure of 3.0 Torr (400 Pa). The flow rates of all gases were determined by direct measurements of the rate of pressure change in calibrated volumes. The overall instrumental error using this system was estimated to be ca. 5%. At each temperature, the dependence of the hydroxyl radical concentration upon the reaction time (the distance between the movable injector and the cavity of the EPR spectrometer) was measured to obtain the first-order decay coefficients for the loss of OH at different concentrations of CH₂ClBr. The bimolecular rate constant k_{CBM} was then calculated from the slope in a plot of τ_{CBM}^{-1} versus [CH₂ClBr].

Experiments were also carried out with a fixed distance between the injector and the detection zone. The dependence of the OH concentration (the EPR signal) versus the concentration of CH₂ClBr was measured to obtain the k_{CBM} value. Under conditions of plug flow, the rate constant is given by

$$k_{\text{CBM}} = -\frac{v}{l} \frac{\partial \ln[\text{OH}]}{\partial [\text{CH}_2\text{ClBr}]}$$

where v is an average flow velocity and l is the distance between the injector and a center of the EPR cavity.

The absorption cross sections for CBM were measured over the wavelength range of 187–290 nm using a double-beam diffraction spectrophotometer.¹⁴ The spectrum was recorded with an increment of 0.1–0.5 nm and a spectral slit width ranging from 0.2 to 1.0 nm. The pressure inside the 14.0 ± 0.05 cm quartz absorption cell, thermostated at 295 ± 1 K, was measured by a bellows inductive manometer with an accuracy of ± 0.01 Torr (1.3 Pa). Absorption spectra of the evacuated cell and of the cell filled with CH₂ClBr were alternately recorded several times and the absorption cross sections calculated from their difference. The spectrum was recorded in three overlapping wavelength ranges. Cross-sections over each of the three ranges were determined from the slopes of a plot of the measured absorbance versus concentration. Typically, four to six concentrations were used for each spectral range. The overall instrumental error resulting from uncertainties in the path length, pressure, temperature, and the measured absorbance was estimated to be less than 2%.

The solubility of CBM in water was estimated from measurements of the change in the UV absorption by both 10 and 2% mixtures of CH₂ClBr in argon. The mixtures were equilibrated in a 5.8 L bulb with 100–460 cm³ of distilled water, which was then pushed out of the bulb and a new portion added for subsequent equilibration. Experiments were performed at ca. 900 Torr (120 kPa) with the 10% mixture and at both 900 Torr (120 kPa) and 300 Torr (40 kPa) with the 2% mixture.

The sample of chlorobromomethane (Aldrich Chemical Co.) used in these studies was analyzed by using GC and GC/MS. The only substantial impurity found was 0.48% CH₂Cl₂. UV analysis of the liquid phase of CBM indicated ca. 6 ppm of Br₂ in the original sample. GC purification was performed to remove the impurities, and less than 0.005% CH₂Cl₂ remained in the purified sample. No absorption band due to molecular bromine was then detected. The same purified sample was used for both measurements of the reaction rate constant as well as for UV absorption cross section measurements.

Results and Discussion

Rate constant measurements by the FP/RF technique employed in this study were complicated by the photolysis of CH₂ClBr by the Xe flash lamp. Hence, experiments were performed at the lowest possible flash energy (corresponding to an electrical energy of approximately 0.4 J) to minimize the possible effects of photofragmentation of CH₂ClBr. Additional experiments, carried out at flash energies ranging over 0.4–4.4 J, showed a

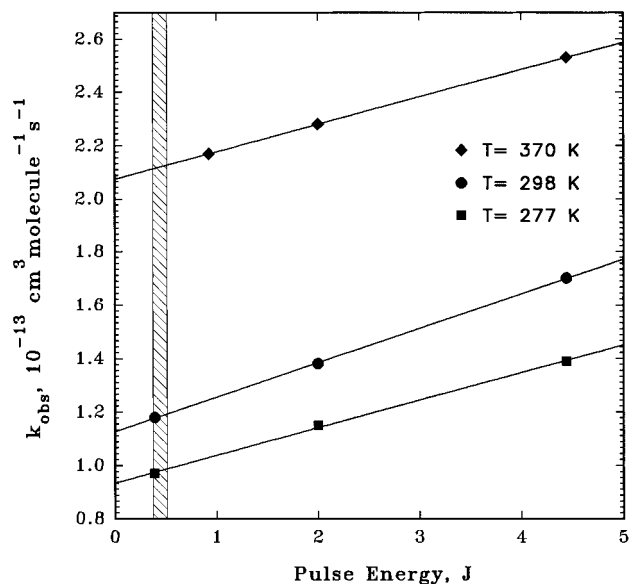


Figure 1. Dependence of the observed rate constant for the reaction of OH with CH₂ClBr on flash energy obtained in FP/RF experiments at 277, 298, and 370 K.

TABLE 1: Rate Constants Measured for the Reaction between OH and Chlorobromomethane

temp, K	$k_{\text{CBM}}, 10^{-13} \text{ cm}^3 \text{ molecule}^{-1} \text{ s}^{-1}$ (no. of expts)	
	FP/RF	DF/EPR
277	0.91 ± 0.10 (2)	
298	1.11 ± 0.06 (4)	1.13 ± 0.06 (4)
313	1.34 ± 0.15 (1)	1.32 ± 0.20 (3)
330	1.58 ± 0.09 (2)	1.55 ± 0.05 (3)
349	1.76 ± 0.25 (3)	1.90 ± 0.17 (3)
370	2.10 ± 0.17 (3)	2.26 ± 0.13 (4)

clear dependence of the observed rate constant ($k_{\text{CBM}}^{\text{obs}}$) on flash energy (Figure 1). From this figure, one can see that even results obtained at the lowest energy were still slightly affected by some “additional chemistry”. Values of $k_{\text{CBM}}^{\text{obs}}$ (298 K) were also measured at the highest flash energy using various total flow rates and flash repetition rates. No dependence of the rate constant on variations of either the total flow rate by a factor of 3 or flash repetition rate by a factor of 10 was discernible. This indicates that any additional chemistry is due to reactions with radicals rather than with stable products accumulating in the reactor.

The values of $k_{\text{CBM}}^{\text{obs}}$ reported here were measured in the low-flash-energy range (indicated by the “shadowed” region in Figure 1) and then slightly corrected using the observed dependence of $k_{\text{CBM}}^{\text{obs}}$ on flash energy. The resultant values of k_{CBM} are presented in Table 1 and Figure 2. Generally, the extrapolation region corresponded to about 9% of the range over which the measurements were performed, resulting in corrections of only 3–6% in the measured values. The following Arrhenius expression for k_{CBM} was derived on the basis of the results of the FP/RF measurements:

$$k_{\text{CBM}}(T) = (2.6_{-0.5}^{+0.6}) \times 10^{-12} \exp\{-(930 \pm 65)/T\} \text{ cm}^3 \text{ molecule}^{-1} \text{ s}^{-1}$$

There are two possible reasons for the observed dependence of the rate of hydroxyl radical loss on flash energy in our FP/RF experiments: (i) a secondary reaction with a radical product of the reaction under study ($R = \text{CHClBr}$) or (ii) reactions with possible radical products of the reactant photolysis ($R_{\text{ph}} = \text{CH}_2\text{Cl}, \text{CH}_2\text{Br}, \text{CH}_2, \text{CHCl}, \text{CHBr}$). In the first case, the OH decay due to chemical reactions can be described as follows:

$$\frac{d[\text{OH}](t)}{dt} = -\{k_{\text{CBM}}[\text{CBM}] + k_{\text{R}}[\text{R}](t)\}[\text{OH}](t)$$

where $[\text{R}](t)$ is a function of the initial concentration of hydroxyl radicals. Note that since k_{R} should have only a slight dependence on temperature, the above equation is essentially the same for any temperature. In our experiments a common range of decay rates (rather than reagent concentrations) was generally used. Therefore, the range of ratios of $\{k_{\text{R}}[\text{R}]/k_{\text{CBM}}[\text{CBM}]\}$ was roughly the same for all experiments. This range depends only on the values of $k_{\text{CBM}}[\text{CBM}]$ and the initial hydroxyl concentration used (i.e., experimental conditions) as well as on the rate constant of the secondary reaction k_{R} (a kinetic condition). Thus, to a first approximation, a secondary reaction involving a radical product from the primary reaction results in the same *relative* overestimation of the rate constant over the temperature range of study. Therefore, with this type of experimental procedure of operating with a common range of decay rates at each temperature, the overestimation of the rate constant due to a secondary reaction should result mainly in an overestimation in the Arrhenius A factor rather than an error in the activation energy.

In the case of reactions between OH and photofragments the OH decay is described by

$$\frac{d[\text{OH}](t)}{dt} = -\{k_{\text{CBM}}[\text{CBM}] + k_{\text{ph}}[\text{R}_{\text{ph}}](t)\}[\text{OH}](t) - \{k_{\text{CBM}}[\text{CBM}] + k_{\text{ph}}[\text{CBM}]/\sigma_{\text{CBM}}\}[\text{OH}](t)$$

where $I\sigma_{\text{CBM}}$ is the integrated coefficient of photodecomposition of CBM. In this case reaction rates of OH with both CBM and photofragments are proportional to the CBM concentration (in contrast with the case discussed above). Such reactions with photofragments result in the same *absolute* overestimation of the rate constant over the temperature range. Therefore, a slope of the plot of $k_{\text{CBM}}^{\text{obs}}$ vs flash energy should be independent of the rate constant (or temperature) as observed in Figure 1. In contrast, in the case of an interference due to a secondary radical reaction (case i), the slope should increase with increasing rate constant or temperature.

Additional experiments were conducted at $T = 277$ K to check the degree to which the measured rate constant depended on the OH concentration alone. Note that for case i discussed above, one would expect such dependence to be large. However, when the initial concentration of OH was increased by a factor of 6.4 (via an increase in H_2O in the carrier gas with both the total gas flow and flash energy (3.3 J) held constant) $k_{\text{CBM}}^{\text{obs}}$ was observed to increase by only about 10%. Therefore, the dependence of $k_{\text{CBM}}^{\text{obs}}$ upon the initial OH concentration alone is about 10–15 times less than the dependence we observed in the experiments using various flash energies (illustrated by Figure 1). (From independent experiments we know that the initial concentration of hydroxyl radicals is also approximately proportional to the flash energy, other experimental conditions being fixed.)

From the above observations we conclude that reactant photolysis is the primary cause for any overestimation of the rate constants in our FP/RF experiments and that our procedure of low-flash-energy operation coupled with a small (well-defined) correction yields values for k_{CBM} that are free from errors associated with OH/radicals reactions.

Results of DF/EPR measurements are also presented in Table 1 and Figure 2. No dependence of the rate constant on the initial OH concentration over the range of 2×10^{11} – 12×10^{11} molecules·cm³ was observed. The following Arrhenius expres-

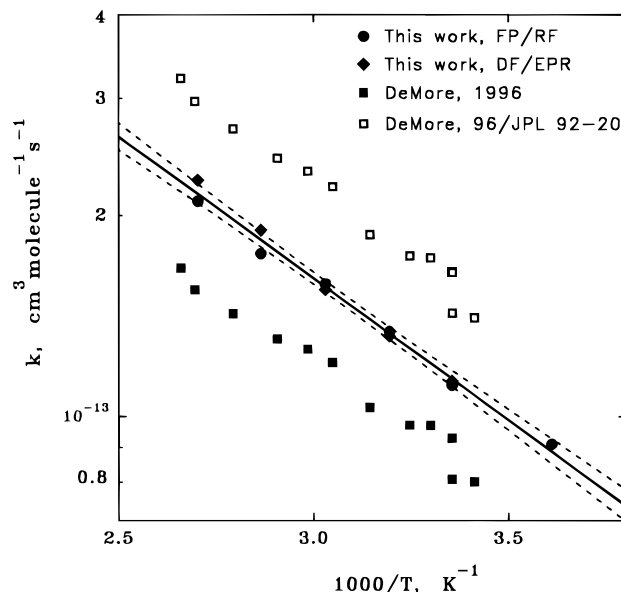


Figure 2. Arrhenius plot of the measured k_{CBM} values and the least-squares fit to both FP/RF and DF/EPR data (solid line) with its statistical 95% confidence intervals (dashed lines). Also plotted are the original result from ref 16 (■) and values rescaled using k_{DCM} from ref 18 (□).

sion for k_{CBM} was derived on the basis of results of DF/EPR measurements:

$$k_{\text{CBM}}(T) = (4.0_{-0.9}^{+1.1}) \times 10^{-12} \exp\{-(1069 \pm 79)/T\} \text{ cm}^3 \text{ molecule}^{-1} \text{ s}^{-1}$$

The results of both the FP/RF and DF/EPR measurements coincide at low temperature and show slight differences (however, within the confidence intervals) above $T = 330$ K. An Arrhenius fit to the combined data sets yields

$$k_{\text{CBM}}(T) = (3.04_{-0.6}^{+0.8}) \times 10^{-12} \exp\{-(978 \pm 72)/T\} \text{ cm}^3 \text{ molecule}^{-1} \text{ s}^{-1}$$

where the error limits are the statistical 95% confidence limits.

For the purpose of atmospheric modeling, the region below room temperature is of the greatest interest. We can rewrite the expression for the rate constant and error limits in the manner chosen by the NASA Panel for Data Evaluation,¹⁵ as we have described previously:¹⁰

$$k_{\text{CBM}}(T) = 1.14 \times 10^{-13} \exp\left\{-978\left(\frac{1}{T} - \frac{1}{298}\right)\right\} \text{ cm}^3 \text{ molecule}^{-1} \text{ s}^{-1}$$

$$\frac{\Delta k(T)}{k(T)} = 0.05 + 0.021 \exp\left\{72\left|\frac{1}{T} - \frac{1}{298}\right|\right\}$$

Here we have included the estimated systematic uncertainty of 5% as well as the statistical uncertainty of 2.1% at $T = 298$ K.

The only other reported measurement of the rate constant for the reaction of OH with CBM is that recently published by DeMore.¹⁶ The rate constant, $k_{\text{CBM}} = 1.8 \times 10^{-12} \exp(-906/T)$, was obtained by a relative rate technique and is based on the author's earlier determination¹⁷ of the rate constant for the reference reaction between OH and CH_2Cl_2 (dichloromethane, DCM). Over the temperature region of overlap, this expression yields rate constants about 30% lower than those reported here. Note, however, that an even higher systematic difference exists between the rate constant for the reference reaction (k_{DCM}) determined by Hsu and DeMore¹⁷ using the relative rate technique and those obtained by several absolute techniques.¹⁸

TABLE 2: Comparison of Rate Constants for CH₃X and CH₂XCl, Where X = F, Cl, Br^a

molecule	A, 10 ⁻¹² cm ³ molecule ⁻¹ s ⁻¹	E/R, K	k(298 K), 10 ⁻¹⁴ cm ³ molecule ⁻¹ s ⁻¹
CH ₃ F	3.0	1500	2.0
CH ₂ FCI	3.0	1250	4.5
CH ₃ Cl	4.0	1400	3.6
CH ₂ Cl ₂	3.8	1050	11.0
CH ₃ Br	4.0	1470	2.9
CH ₂ BrCl	3.1	990	11.4

^a All parameters are taken from ref 15 with the exception of those for CH₂ClBr, which are taken from the present work.

Combining the rate constants ratios obtained by DeMore¹⁶ ($k_{\text{CBM}}/k_{\text{DCM}}$) with a recommended value¹⁸ for k_{DCM} which is based only on the absolute results, one can derive $k_{\text{CBM}} = 4.8 \times 10^{-12} \exp(-1025/T)$. This expression yields values for k_{CBM} that are 35–40% higher than those obtained in the present work. Both the original and rescaled results from ref 16 are presented in Figure 2 along with the results from the present study.

It is not clear whether the differences between the k_{CBM} values from the present study and those from ref 16 are due to unresolved errors in either of the studies or to remaining uncertainties in k_{DCM} . This later uncertainty can be seen from the following exercise. Using the value for k_{CBM} determined from our absolute measurements, one can calculate k_{DCM} from the $k_{\text{CBM}}/k_{\text{DCM}}$ ratios obtained by DeMore.¹⁶ Thus we obtain

$$k_{\text{DCM}}(T) = (3.6_{-1.0}^{+1.5}) \times 10^{-12} \exp\{-(1050 \pm 110)/T\} \text{ cm}^3 \text{ molecule}^{-1} \text{ s}^{-1}$$

where the error limits are the statistical 95% confidence limits due to data¹⁶ scattering only. This expression lies between most of the previous absolute determinations¹⁸ and that recently obtained by the relative technique.¹⁷ Coincidentally, the latest recommendation¹⁵ for k_{DCM} (taken simply as a mean from the relative and absolute measurement studies) is nearly the same as the above result.

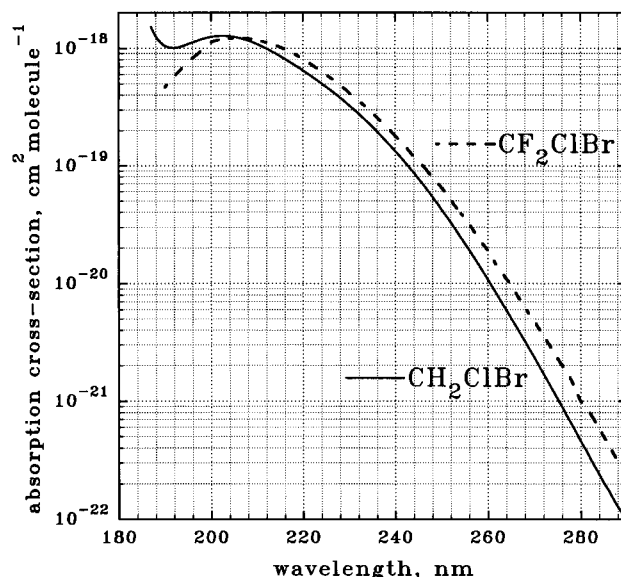
An additional observation can be made using these rate constants. In Table 2 we have listed the Arrhenius parameters and room temperature rate constants for CH₃F, CH₃Cl, and CH₃-Br as well as the three compounds derived by replacing an H atom with a Cl atom. As can be seen from this series, the room temperature rate constant increases in each case (by factors of 2.2–3.9) and this increase appears to be due almost entirely to a reduction in the Arrhenius E/R of 250–500 K. Thus, chlorine substitution in these monomethyl halides increases the reactivity of the remaining two H atoms by a reduction in the C–H bond strength.

The UV spectrum of CBM has a maximum cross-section, $\sigma = 1.27 \times 10^{-18} \text{ cm}^2$, at $\lambda = 202.6 \pm 0.5 \text{ nm}$ and shows a rising absorption as λ decreases below 192 nm. The absorption cross-sections for CH₂ClBr are listed in Table 3 and plotted in Figure 3 along with that of CF₂ClBr for comparison.¹⁵

The effect of liquid water being added to a bulb containing a CBM/Ar mixture was easily measurable. A near 40% decrease in the gas-phase CBM concentration was observed in the presence of 120 cm³ of water. No dependence on either the abundance of CH₂ClBr in the mixture or on the total gas pressure in the bulb was observed. We can estimate an Ostwald solubility coefficient (*S*) from the following equation:

$$S = \frac{V_g}{\nu_w} \left(\frac{[\text{CBM}]_0}{[\text{CBM}]_w} - 1 \right)$$

where V_g and ν_w are the volumes of bulb and liquid water and $[\text{CBM}]_0$ and $[\text{CBM}]_w$ are the measured concentrations of CH₂-

**Figure 3.** Ultraviolet absorption cross-sections of CH₂ClBr (solid line) and CF₂ClBr (dashed line) at $T = 295 \text{ K}$.**TABLE 3: Absorption Cross-Sections of CH₂ClBr at $T = 295 \text{ K}$**

λ , nm	σ , 10 ⁻²⁰ cm ²	λ , nm	σ , 10 ⁻²⁰ cm ²	λ , nm	σ , 10 ⁻²⁰ cm ²
187	151.1	210	108.4	246	6.94
188	126.4	211	104.0	248	5.46
189	112.5	212	99.6	250	4.24
190	104.6	213	95.0	252	3.29
191	101.6	214	90.5	254	2.52
192	100.5	215	85.9	256	1.92
193	102.0	216	81.5	258	1.45
194	104.7	217	77.1	260	1.09
195	108.4	218	72.9	262	0.807
196	111.8	219	68.8	264	0.596
197	115.7	220	64.8	266	0.440
198	119.4	222	57.4	268	0.322
199	122.3	224	50.5	270	0.235
200	124.7	226	44.1	272	0.170
201	126.3	228	38.2	274	0.123
202	127.1	230	32.8	276	0.089
203	127.1	232	28.0	278	0.064
204	126.3	234	23.6	280	0.046
205	124.7	236	19.7	282	0.033
206	122.5	238	16.3	284	0.024
207	119.7	240	13.4	286	0.0178
208	116.3	242	10.8	288	0.0129
209	112.6	244	8.73	290	0.0098

ClBr without and with water in the bulb, respectively. Thus, we obtained $S \approx 19$ for CBM in distilled water at $T = 295 \text{ K}$.

Atmospheric Implications

Reactions with hydroxyl radicals in the troposphere are the main removal processes for hydrohalocarbons. The atmospheric lifetime of CBM (τ_{CBM}) can, therefore, be estimated by a simple scaling procedure. Following Prather and Spivakovsky,¹⁹ we can estimate the lifetime of CBM due to reactions with hydroxyl radicals in the troposphere as

$$\tau_{\text{CBM}}^{\text{OH}} = \frac{k_{\text{MC}}(277 \text{ K})}{k_{\text{CBM}}(277 \text{ K})} \tau_{\text{MC}}^{\text{OH}}$$

where $\tau_{\text{CBM}}^{\text{OH}}$ and $\tau_{\text{MC}}^{\text{OH}}$ are the atmospheric lifetimes of CBM and methylchloroform (MC), respectively, due to reactions with hydroxyl radicals in the troposphere, and $k_{\text{CBM}}(277 \text{ K})$, $k_{\text{MC}}(277 \text{ K}) = 6.69 \times 10^{-15} \text{ cm}^3 \text{ molecule}^{-1} \text{ s}^{-1}$ ¹⁵ are the rate constants for the reactions of OH with these substances at $T = 277 \text{ K}$. The total atmospheric lifetime of methylchloroform has

been derived from measurements of trends in its concentration in the atmosphere to be $\tau_{MC} = 4.8$ years.²⁰ A correction for both the ocean loss²¹ and photolysis in the stratosphere^{22,23} must be done to estimate τ_{MC}^{OH} from τ_{MC} :

$$\frac{1}{\tau_i} = \frac{1}{\tau_i^{OH}} + \frac{1}{\tau_i^{ph}} + \frac{1}{\tau_i^{ocean}}$$

Here τ_i^{ph} and τ_i^{ocean} are the characteristic times for substance losses from the atmosphere due to photolysis and due to ocean removal (which are ca. 45 years^{22,23} and ca. 85 years,²¹ respectively, in the case of MC). Such estimations result in $\tau_{MC}^{OH} = 5.7$ years, $\tau_{CBM}^{OH} = 0.43$ years.

Following the procedure described in refs 4 and 23, we can estimate τ_{CBM}^{ocean} on the basis of its water solubility, assuming that dissolution in the ocean leads to chemical degradation. For this estimate, we have taken the parameters used for the estimation of the atmospheric lifetime of CH_3Br due to ocean removal,^{4,24} along with the Ostwald solubility coefficient for CH_2ClBr estimated in this work. This results in a value of τ_{CBM}^{ocean} of approximately 0.42 years, which should be considered a lower limit. This leads to a revised estimate for the atmospheric lifetime of $\tau_{CBM} = 0.21$ years (compared to 0.43 years due to reaction with OH only). Note that solubility is only the first step in an oceanic removal process. In the absence of relatively fast processes for chemical decomposition, the ocean will act simply as a temporary reservoir, not as a sink. Nevertheless, it is clear that the existence of an oceanic sink can noticeably affect the atmospheric lifetime of CBM and the study of chemical degradation rates of CH_2ClBr in sea water may be warranted.

Dissociation by solar UV radiation has only a minor effect on the atmospheric lifetime of CBM. This can be seen from a comparison with CF_2ClBr . Photodissociation in the troposphere is the main removal process for CF_2ClBr , which has an estimated lifetime of 20 years.⁴ Absorption cross-sections for CH_2ClBr are a factor of 2.0–2.4 smaller than those for CF_2ClBr in the long-wavelength tail where tropospheric photodissociation can become important. Therefore, τ_{CBM}^{ph} should be approximately twice as long as that for CF_2ClBr (quantum yield of photodissociation has been taken as unity in both cases), and photodissociation contributes only about 1% to the total atmospheric removal of CBM.

Finally, we can also estimate the ozone depletion potential (ODP) of CBM on the basis of both its estimated lifetime and the calculated ODPs for other Br containing substances. Taking CH_3Br (lifetime = 1.3 years, ODP = 0.6)⁴ and CF_2ClBr (lifetime = 20 years, ODP = 5)⁴ as reference species, we can use a scaling procedure to account for differences in lifetimes and molecular weights:

$$ODP(CBM) = ODP(i) \frac{\tau_{CBM}}{\tau_i} \frac{M_i}{M_{CBM}}$$

where $ODP(CBM)$, $ODP(i)$, τ_{CBM} , τ_i , M_{CBM} , and M_i are ODPs, atmospheric lifetimes, and molecular weights of chlorobromomethane and a reference substance, respectively. Both estimates result in an $ODP \approx 0.14$ for $\tau_{CBM}^{OH} = 0.43$ years due to reaction with tropospheric hydroxyl only and decrease to an $ODP \approx 0.07$ for $\tau_{CBM} = 0.21$ years under the assumption of a fast oceanic removal.

Note that the above estimations of lifetimes and ODPs assume a uniformly distributed gas over the troposphere. For a compound with a short lifetime, such as CH_2ClBr , this assumption is probably not valid globally and more comprehensive modeling calculations are required. To illustrate this, we

mention here the results of calculations performed for CH_2Br_2 .²⁵ This substance has the same reactivity toward OH as CH_2ClBr , resulting in an atmospheric lifetime as short as 0.40 years.²⁵ Calculations using a coupled dynamical/chemical two-dimensional model of the atmosphere resulted in approximately a 25% lower ODP value in comparison with that deduced from a scaling procedure similar to that used in the present paper. Nonuniform distribution of the substance over the troposphere was cited as being the cause of this difference.

Acknowledgment. This work was funded by the Upper Atmosphere Research Program of the National Aeronautics and Space Administration and by the U.S. Army Research Laboratory through MIPR 6F-ARL-80115. We would like to thank Mr. L. Clark (Enviro Tech International) for his suggestions regarding the initiation of this study and for financial support of the studies done in Moscow. The work done in the Institute of Energy Problems of Chemical Physics was funded in part by the Russian Basic Research Foundation under Grant 96-05-65477.

References and Notes

- (1) *Scientific Assessment of Stratospheric Ozone*, 1989; Global Ozone Research and Monitoring Project, Report No. 20; World Meteorological Organization: 1989; Vol. I.
- (2) Rasmussen, R. A.; Khalil, M. A. K. *Geophys. Res. Lett.* **1984**, *11*, 433–436.
- (3) Class, T. H.; Ballschmiter, K. *J. Atmos. Chem.* **1988**, *6*, 35–46.
- (4) *Scientific Assessment of Ozone Depletion*, 1994; Global Ozone Research and Monitoring Project, Report No. 37; World Meteorological Organization: 1995; p 10.13.
- (5) Clark, L. Enviro Tech International, personal communication.
- (6) Kurylo, M. J.; Cornett, K. D.; Murphy, J. L. *J. Geophys. Res.* **1982**, *87*, 3081–3085.
- (7) Wallington, T. J.; Neuman, D. M.; Kurylo, M. J. *Int. J. Chem. Kinet.* **1987**, *19*, 725–739.
- (8) Liu, R.; Huie, R. E.; Kurylo, M. J. *J. Phys. Chem.* **1990**, *94*, 3247–3249.
- (9) Zhang, Z.; Padmaja, S.; Saini, R. D.; Huie, R. E.; Kurylo, M. J. *J. Phys. Chem.* **1994**, *98*, 4312–4315.
- (10) Orkin, V. L.; Huie, R. E.; Kurylo, M. J. *J. Phys. Chem.* **1996**, *100*, 8907–8912.
- (11) Orkin, V. L.; Khamaganov, V. G. *J. Atmos. Chem.* **1993**, *16*, 157–167.
- (12) Orkin, V. L.; Khamaganov, V. G.; Larin, I. K. *Int. J. Chem. Kinet.* **1993**, *25*, 67–78.
- (13) Orkin, V. L.; Khamaganov, V. G. *J. Atmos. Chem.* **1993**, *16*, 169–178.
- (14) Orkin, V. L.; Kasimovskaya, E. E. *J. Atmos. Chem.* **1995**, *21*, 1–11.
- (15) DeMore, W. B.; Sander, S. P.; Golden, D. M.; Hampson, R. F.; Kurylo, M. J.; Howard, C. J.; Ravishankara, A. R.; Kolb, C. E.; Molina, M. J. *JPL Publ.* **1994**, 94-26.
- (16) DeMore, W. B. *J. Phys. Chem.* **1996**, *100*, 5813–5820.
- (17) Hsu, K.-J.; DeMore, W. B. *Geophys. Res. Lett.* **1994**, *21*, 805–808.
- (18) DeMore, W. B.; Sander, S. P.; Golden, D. M.; Hampson, R. F.; Kurylo, M. J.; Howard, C. J.; Ravishankara, A. R.; Kolb, C. E.; Molina, M. J. *JPL Publ.* **1992**, 92-20.
- (19) Prather, M.; Spivakovsky, C. M. *J. Geophys. Res.* **1990**, *95*, 18723–18729.
- (20) Prinn, R. G.; Weiss, R. F.; Miller, B. R.; Huang, J.; Alyea, F. N.; Cunnold, D. M.; Fraser, P. J.; Hartley, D. E.; Simmonds, P. G. *Science* **1995**, *269*, 187–192.
- (21) Butler, J. H.; Elkins, J. W.; Thompson, T. M.; Ball, B. D.; Swanson, T. H.; Koropalov, V. *J. Geophys. Res.* **1991**, *96*, 22347–22355.
- (22) Kaye, J. A.; Penkett, S. A.; Ormond, F. M. *NASA Ref. Publ.* **1994**, 1339.
- (23) *Proceedings of the Workshop on the Atmospheric Degradation of HFCs and HCFCs*, Boulder, CO, 1993.
- (24) Butler, J. H. *Geophys. Res. Lett.* **1994**, *21*, 185–188.
- (25) Mellouki, A.; Talukdar, R. K.; Schmoltnner, A.-M.; Gierczak, T.; Mills, M. J.; Solomon, S.; Ravishankara, A. R. *Geophys. Res. Lett.* **1992**, *19*, 2059–2062.
- (26) Certain commercial equipment, instruments, or materials are identified in this article in order to adequately specify the experimental procedure. Such identification does not imply recognition or endorsement by the National Institute of Standards and Technology, nor does it imply that the material or equipment identified are necessarily the best available for the purpose.